# Matrix formalism for calculation of electric field intensity of light in stratified multilayered films

Koji Ohta and Hatsuo Ishida

A new algorithm has been proposed for the calculation of the electric field intensity in stratified multilayered films when light is incident on the system. The algorithm utilizes matrix formulas based on Abeles's formulas for the calculation of reflectance and transmittance. Equations for calculating patial absorptance due to a certain depth in the films are also derived. Some examples of the application of the electric field description are given for the analysis of three kinds of reflection spectroscopic methods which use metal surfaces: reflection–absorption, surface electromagnetic wave, and metal overlayer ATR methods. The algorithm given here offers a useful tool in understanding the mechanism of light absorption in various spectroscopic methods, and is convenient to use where intensity of the IR spectrum is of interest.

## I. Introduction

The profile of the electric field intensity for light incident on a multilayered system has played an important role in the analysis of various kinds of spectroscopy, especially reflection spectroscopy. Fry[1] first depicted the variation of the electric field intensity at the surface of metals vs the incident angle of the light. Later, Francis and Ellison[2] used the same picture to explain the mechanism of the enhancement of absorption of thin films on a metal at the grazing angle of incidence. This method, which we call reflection–absorption (RA) spectroscopy today, has been widely used for analysis of thin films or adsorbents on metals. For attenuated total reflection (ATR) spectroscopy, Harrick[3] explained that penetration of the evanescent wave into the surface of the sample governs the absorption of the light in terms of electric field strength. He also showed how to calculate, from the electric fields, the energy absorbed from the surface to a certain depth. Using this picture, we have been able to estimate the fraction of the contribution of the surface layer to the total absorption.[4] The applications of electric field description to spectroscopy in its early stages are well documented in two reviews.[5,6] Lately, electric field analysis has been used extensively to explain the mechanism of ellipsometry,[7] exciton surface polariton,[8,9] metal surface Raman,[10] enhancement of IR absorption,[11] metal overlayer ATR spectroscopy,[12] and surface electromagnetic wave (SEW) spectroscopy.[13,14]

Hansen[15] derived a method for calculating the light electric field at an arbitrary depth for stratified films with $N$ phase using a matrix method[16] in terms of the electric field E and magnetic field $H$, which includes the calculation of inversion of the matrices. This report introduces a new algorithm to calculate the electric field intensities for stratified films with any number of phases, which does not require the calculation of inverse matrices. This method is based on the Abele's matrix method[17] in terms of forward and backward propagating electric fields, that is, $E^+$ and $E^-$, which were introduced to calculate the reflectance and transmittance of the light. The results from our method are equivalent to those from Hansen's method. However, our method has several advantages; it is more computer-tractable, and the calculation can be done within almost the same time as they required for calculation of the reflectance and transmittance by using the same framework. Moreover, this method can be extended to a system with phase incoherence. In the succeeding paper, we will describe the extension of this method to the incoherent layers in detail.[18] A possible way to calculate partial absorptance will also be shown together with its application to the analysis of emission spectra. Several equations derived here include, as special cases, other equations that were used for more limited systems. The present matrix formulation of

When this work was done both authors were with Case Western Reserve University, Department of Macromolecular Science, Cleveland, Ohio 44106; K. Ohta has now returned to Government Industrial Research Institute of Osaka, Midorigaoka, Ikeda, Osaka 563, Japan.

Received 26 February 1988.
0003-6935/90/131952-08$02.00/0.

light propagation offers a powerful tool for the analysis of results obtained from various kinds of spectroscopic methods.

## II. Abeles' Matrix Method

The method that we introduce here for calculating the intensity of the electric field is based on Abeles's matrix method[17] using $E^+$ and $E^-$ as basis vectors used for calculation of reflectance and transmittance. Since Heavens[19] described Abeles's method concisely, and Azzam and Bashara[20] reformulated the equations in a more elegant manner, we will follow hereafter their notation and coordinate system in introducing all equations except for the following equation which we adopt for the complex refractive index:

$$\hat{n}_j = n_j + ik_j. \tag{1}$$

The optical configuration used in the present study is described in Fig. 1. Abeles showed that the relation among the amplitudes of the electric fields of incident wave $E_0^+$, reflected wave $E_0^-$, and transmitted wave after $m$ layers $E_{m+1}^+$ is expressed as the following matrix equation for stratified films with $m$ layers.

$$\begin{pmatrix} E_0^+ \\ E_0^- \end{pmatrix} = \frac{C_1 C_2 \dots C_{m+1}}{t_1 t_2 \dots t_{m+1}} \begin{pmatrix} E_{m+1}^+ \\ E_{m+1}^- \end{pmatrix}. \tag{2}$$

here, $C_j$ is the propagation matrix with the matrix elements

$$C_j = \begin{pmatrix} \exp(-i\delta_{j-1}) & r_j \exp(-i\delta_{j-1}) \\ r_j \exp(i\delta_{j-1}) & \exp(i\delta_{j-1}) \end{pmatrix}, \tag{3}$$

where $t_j$ and $r_j$ are the Fresnel transmission and reflection coefficients, respectively, between the $(j-1)$-th and $j$-th layers. The Fresnel coefficients $t_j$ and $r_j$ can be expressed as follows by using the complex refractive index $\hat{n}_j$ and the complex refractive angle $\theta_j$: for parallel ($p$) polarization

$$r_{jp} = \frac{\hat{n}_{j-1}\cos\theta_j - \hat{n}_j \cos\theta_{j-1}}{\hat{n}_{j-1}\cos\theta_j + \hat{n}_j \cos\theta_{j-1}} \tag{4}$$

$$t_{jp} = \frac{2\hat{n}_{j-1}\cos\theta_{j-1}}{\hat{n}_{j-1}\cos\theta_j + \hat{n}_j \cos\theta_{j-1}} \tag{5}$$

and for perpendicular ($s$) polarization

$$r_{js} = \frac{\hat{n}_{j-1}\cos\theta_{j-1} - \hat{n}_j \cos\theta_j}{\hat{n}_{j-1}\cos\theta_{j-1} + \hat{n}_j \cos\theta_j} \tag{6}$$

$$t_{js} = \frac{2\hat{n}_{j-1}\cos\theta_{j-1}}{\hat{n}_{j-1}\cos\theta_{j-1} + \hat{n}_j \cos\theta_j}. \tag{7}$$

The complex refractive indices and the complex angles of incidence obviously follow Snell's law

$$\hat{n}_{j-1}\sin\theta_{j-1} = \hat{n}_j \sin\theta_j \qquad (j = 1, 2, \dots, m+1) \tag{8}$$

The values $\delta_{j-1}$ in Eq. (3) indicate the change of phase of the wave between the $(j-1)$-th and $j$-th boundaries and are expressed by the equations:

$$\delta_0 = 0 \tag{9}$$

$$\delta_{j-1} = 2\pi\nu\hat{n}_{j-1}\cos\theta_{j-1}h_{j-1} \tag{10}$$

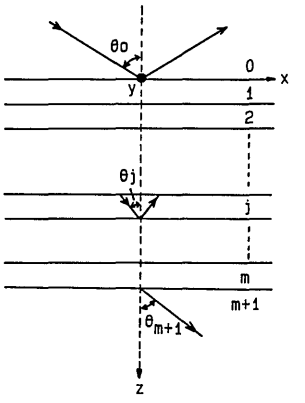


Fig. 1. Coordinate system and notation of the number of the films for the present stratified multilayered film system. The film structure is sandwiched between the incident (0) and substrate ($m+1$) phases.

except for $j = 1$, where $\nu$ is the wavenumber of the incident light in vacuum and $h_{j-1}$ means the thickness of the $(j-1)$-th layer.

By putting $E_{m+1}^- = 0$ because there is no reflection from the final phase, Abeles[17] obtained a convenient formula for the total reflection and transmission coefficients which correspond to the amplitude reflectance $r$ and transmittance $t$, respectively, as follows:

$$r = \frac{E_0^-}{E_0^+} = \frac{c}{a} \tag{11}$$

$$t = \frac{E_{m+1}^+}{E_0^+} = \frac{t_1 t_2 \dots t_{m+1}}{a}, \tag{12}$$

where the quantities $a$ and $c$ are the matrix elements of the product of all $C_j$ matrices:

$$C_1 C_2 C_3 \dots C_{m+1} = \begin{pmatrix} a & b \\ c & d \end{pmatrix}. \tag{13}$$

By using Eqs. (11) and (12), we can easily obtain energy reflectance $R$ as

$$R = |r|^2 \tag{14}$$

for both polarizations, and the energy transmittance $T$ as

$$T_s = \mathrm{Re}\left(\frac{\hat{n}_{m+1}\cos\theta_{m+1}}{\hat{n}_0\cos\theta_0}\right)|t_s|^2, \tag{15}$$

$$T_p = \mathrm{Re}\left(\frac{\cos\theta_{m+1}/\hat{n}_{m+1}}{\cos\theta_0/\hat{n}_0}\right)\left|\frac{\hat{n}_{m+1}}{\hat{n}_0}t_p\right|^2$$

$$= \mathrm{Re}\left(\frac{\hat{n}_{m+1}^*\cos\theta_{m+1}}{\hat{n}_0^*\cos\theta_0}\right)|t_p|^2, \tag{16}$$

for $s$- and $p$-polarization, respectively, where Re indicates the real part of. In particular, when the final phase is light absorbing at the relevant wavenumber, this energy transmittance means the energy fraction of the light penetrating into the final phase and absorbed there.

## III. Electric Field Calculation

First we show the equation for calculating the light electric fields at the boundaries. Then, we obtain the electric fields at an arbitrary depth $z$ from the surface of the stratified films. For this purpose, we divide Eq. (2) into two parts:

$$\begin{pmatrix} E_0^+ \\ E_0^- \end{pmatrix} = \frac{C_1 C_2 \dots C_j}{t_1 t_2 \dots t_j} \begin{pmatrix} E_j^+ \\ E_j^- \end{pmatrix} \tag{17}$$

$$\begin{pmatrix} E_j^+ \\ E_j^- \end{pmatrix} = \frac{C_{j+1} C_{j+2} \dots C_{m+1}}{t_{j+1} t_{j+2} \dots t_{m+1}} \begin{pmatrix} E_{m+1}^+ \\ E_{m+1}^- \end{pmatrix}. \tag{18}$$

These equations $E_j^+$ and $E_j^-$, respectively, are the amplitudes of the forward and backward propagating waves of the light infinitesimally below the $j$-th boundary except for $E_0^+$ and $E_0^-$. $E_0^+$ and $E_0^-$ are the respective amplitudes of the incident and reflected waves infinitesimally above the first boundary, that is, the surface of the films. We can obtain the relationships between $E_0^+$ and $E_j^+$, or $E_0^+$ and $E_j^-$ from Eq. (17) only by using the inverse matrix of the product $C_1 C_2 \dots C_j$, since the relationship between $E_0^+$ and $E_0^-$ was already obtained in Eq. (11). This method was suggested by Swalen and Rabolt.[21] However, we do not need to use the inverse matrix if first we express $E_j^+$ and $E_j^-$ in terms of Eq. (18), and then we express them in terms of $E_0^+$ from Eq. (12). For convenience, we define the matrices $D_j$ as the product of $C_{j+1} C_{j+2} \dots C_{m+1}$.

$$D_j = C_{j+1} C_{j+2} \dots C_{m+1} = \begin{pmatrix} a_j & b_j \\ c_j & d_j \end{pmatrix}. \tag{19}$$

From $E_{m+1}^- = 0$ in Eq. (18), $E_j^+$ is expressed by the (1,1) element $a_j$ of the $D_j$ matrix and $E_{m+1}^+$, and $E_j^-$ by the (2,1) element $c_j$ and $E_{m+1}^+$ as follows:

$$E_j^+ = \frac{a_j}{t_{j+1} t_{j+2} \dots t_{m+1}} E_{m+1}^+ \tag{20}$$

$$E_j^- = \frac{c_j}{t_{j+1} t_{j+2} \dots t_{m+1}} E_{m+1}^+. \tag{21}$$

Substitution of $E_{m+1}^+$ in Eqs. (20) and (21) by Eq. (12) gives the following two equations:

$$E_j^+ = t_1 t_2 \dots t_j \frac{a_j}{a} E_0^+ \tag{22}$$

$$E_j^- = t_1 t_2 \dots t_j \frac{c_j}{a} E_0^+ \tag{23}$$

Thus we obtain the equations for relationships between $E_j^+$ and $E_0^+$, and $E_j^-$ and $E_0^+$.

We describe advantages of the above method as follows. The quantities that appear in Eqs. (22) and (23) are the (1,1) element for Eq. (22), the (2,1) element for Eq. (23) of the $D_j$ matrix, and the product of Fresnel transmission coefficients from the first to the $j$-th boundaries $t_1 t_2 \dots t_j$ for both equations. These quantities can all be calculated while obtaining the total reflectance and transmittance of stratified multilayered films, which make use of Eqs. (11), (12), and (13). The product from $t_1$ to $t_j$ is obtainable in the course of successive multiplication for the product from $t_1$ to $t_{m+1}$, which appears in Eq. (12). Moreover, the matrix elements of $D_j$ can be obtained in the course of successive multiplication for the product of all the $C_j$ matrix, the (1,1) and (2,1) elements of which appear in Eqs. (11) and (12), if we begin the multiplication from $C_{m+1}$ instead of $C_1$. Therefore, using the present $D_j$ matrix formulas, we do not have to make the calculation of the inverse matrices, which were suggested by Hansen[15] or Swalen and Rabolt.[21] The computer program can be readily coded as long as the language used can deal with complex numbers. Therefore, Eqs. (22) and (23) are very convenient formulas for calculating the field amplitude at each boundary because we can complete the calculation of the value within almost the same time as required for the calculation of the reflectance and transmittance when we use Eqs. (11), (12), and (13).

When $j = 0$,

$$D_0 = C_1 C_2 \dots C_{m+1} = \begin{pmatrix} a & b \\ c & d \end{pmatrix}. \tag{24}$$

Eq. (23) is then reduced to Eq. (11) which expresses the reflection coefficient of the stratified multilayered system. It is convenient to define $D_{m+1}$ as a unit matrix:

$$D_{m+1} = \begin{pmatrix} 1 & 0 \\ 0 & 1 \end{pmatrix}. \tag{25}$$

Then, Eq. (22) is reduced to Eq. (12) expressing the transmission coefficient of the whole films. Moreover, since the (2,1) element $c_{m+1}$ of $D_{m+1}$ matrix is equal to zero in this case, the equation

$$E_{m+1}^- = 0, \tag{26}$$

is naturally derived from Eq. (23) without any assumptions.

Next, we show the formula for the intensity of each component of the electric field at an arbitrary depth $z$. The amplitude $E(z)$ is expressed as the superposition of the forward propagating wave $E^+(z)$ and the backward propagating wave $E^-(z)$. $E^+(z)$ and $E^-(z)$ are expressed by the amplitudes at the interface $E_j^+$ and $E_j^-$ as

$$E^+(z) = E_j^+ \exp(iK_{zj}\Delta z), \tag{27}$$

$$E^-(z) = E_j^- \exp(-iK_{zj}\Delta z), \tag{28}$$

where $j$ is the number of the phase to which the depth $z$ belongs, $K_{zj}$ is the $z$-component of the wave vector:

$$K_{zj} = 2\pi\nu\hat{n}_j \cos\theta_j \tag{29}$$

and $\Delta z$ is the distance from the $j$-th boundary:

$$\Delta z = z - \sum_{i=1}^{j-1} h_i. \tag{30}$$

When we consider each component of electric field vector $E_x(z)$, $E_y(z)$, or $E_z(z)$, we have to designate the distinction of the polarization explicitly.

$$E_x(z) = [E_p^+(z) - E_p^-(z)] \cos\theta_j \tag{31}$$

$$E_y(z) = E_s^+(z) + E_s^-(z) \tag{32}$$

$$E_z(z) = [E_p^+(z) + E_p^-(z)] \sin\theta_j. \tag{33}$$

The signs for the superposition can change according to the choice of the coordinate system.

Field intensities $F(z)$ are usually defined as the ratio of the square of the amplitudes of the field $|E(z)|^2$ to that of the incident field $|E_0^+|^2$ of each polarization, $|E_{op}^+|^2$ and $|E_{os}^+|^2$:

$$F_x(z) = |E_x(z)|^2/|E_{op}^+|^2 \tag{34}$$

$$F_y(z) = |E_y(z)|^2/|E_{os}^+|^2 \tag{35}$$

$$F_y(z) = |E_z(z)|^2/|E_{op}^+|^2 \tag{36}$$

The intensities of the light fields polarized perpendicularly and parallel to the plane of incidence are, respectively,

$$F_s(z) = F_y(z) \tag{37}$$

$$F_p(z) = F_x(z) + F_z(z). \tag{38}$$

If we define the index of polarization as the ratio of intensity of the parallel polarized light to the total light intensity in the incident light as $X$,

$$X = |E_{op}^+|^2/(|E_{op}^+|^2 + |E_{os}^+|^2), \tag{39}$$

followed by

$$1 - X = |E_{os}^+|^2/(|E_{op}^+|^2 + |E_{os}^+|^2), \tag{40}$$

and then, the total field intensity of the light at the depth $z$ is

$$\begin{aligned} F(z) &= [|E_x(z)|^2 + |E_y(z)|^2 + |E_z(z)|^2]/[|E_{op}^+|^2 + |E_{os}^+|^2) \\ &= XF_p(z) = (1 - X)F_s(z) \\ &= X[F_x(z) + F_z(z)] + (1 - X)F_y(z). \end{aligned} \tag{41}$$

When there is no polarization in the incident light, $X = 1/2$ and then,

$$F(z) = [F_x(z) + F_y(z) + F_z(z)]/2. \tag{42}$$

In Tables I, II, and III, we show the explicit equations of the $D_j$ matrices, the relationships between $E_0^+$ and $E_j^\pm$, and the electric fields $F(z)$, respectively, derived from our matrix method for the three-phase system. In Table III,

$$\begin{aligned} \beta_2 &= 2\,\mathrm{Im}(K_{z2}) \\ &= 4\pi\nu\,\mathrm{Im}(\hat{n}_2 \cos\theta_2), \end{aligned} \tag{43}$$

where Im denotes the imaginary part of. These formulas are all equivalent to those proposed previously for the three-phase system by Bashara and Peterson,[7] Hansen,[15] and Johnson and Peterson.[22] We can calculate the matrix formulas with numerical values for the Fresnel coefficients of each interface, we do not need the explicit formulas in the actual calculations.

**Table I. Explicit Formulas of $D_j$ Matrices for the Cases of Three-Phase System.**

$$D_2 = \begin{pmatrix} 1 & 0 \\ 0 & 1 \end{pmatrix}$$

$$D_1 = C_2 = \begin{pmatrix} \exp(-i\delta_1) & r_2 \exp(-i\delta_1) \\ r_2 \exp(i\delta_1) & \exp(i\delta_1) \end{pmatrix}$$

$$D_0 = C_1 C_2 = \begin{pmatrix} \exp(-i\delta_1)+r_1r_2\exp(i\delta_1) & r_2\exp(-i\delta_1)+r_1\exp(i\delta_1) \\ r_1\exp(-i\delta_1)+r_2\exp(i\delta_1) & r_1r_2\exp(-i\delta_1)+\exp(i\delta_1) \end{pmatrix}$$

## IV. Absorptance Formulas Using Electric Field Expressions

The electric field description of the light has another advantage that the contribution of the energy absorbed at a certain thickness to the total absorptance

**Table II. Explicit Formulas of the Relationships Between $E_0^+$ and $E_j^\pm$ for the Case of Three-Phase System.**

$$E_0^- = \frac{r_1 \exp(-i\delta_1) + r_2 \exp(i\delta_1)}{\exp(-i\delta_1) + r_1 r_2 \exp(i\delta_1)} E_0^+ = r E_0^+$$

$$E_1^+ = \frac{t_1 \exp(-i\delta_1)}{\exp(-i\delta_1) + r_1 r_2 \exp(i\delta_1)} E_0^+$$

$$E_1^- = \frac{t_1 r_2 \exp(i\delta_1)}{\exp(-i\delta_1) + r_1 r_2 \exp(i\delta_1)} E_0^+$$

$$E_2^+ = \frac{t_1 t_2}{\exp(-i\delta_1) + r_1 r_2 \exp(i\delta_1)} E_0^+ = t E_0^+$$

**Table III. Explicit Formulas of Each Component of Electric Field $F(z)$ for the Case of Three-Phase System.**

The incident (0) phase.

$$F_x(z) = \left|\exp(iK_{zo}z) - \frac{r_{1p}\exp(-i\delta_1)+r_{2p}\exp(i\delta_1)}{\exp(-i\delta_1)+r_{1p}r_{2p}\exp(i\delta_1)} \exp(-iK_{zo}z)\right|^2 \cos^2\theta_o$$

$$= |\exp(iK_{zo}z) - r_p \exp(-iK_{zo}z)|^2 \cos^2\theta_o$$

$$F_y(z) = \left|\exp(iK_{zo}z) + \frac{r_{1s}\exp(-i\delta_1)+r_{2s}\exp(i\delta_1)}{\exp(-i\delta_1)+r_{1s}r_{2s}\exp(i\delta_1)} \exp(-iK_{zo}z)\right|^2$$

$$= |\exp(iK_{zo}z) + r_s \exp(-iK_{zo}z)|^2$$

$$F_z(z) = \left|\exp(iK_{zo}z) + \frac{r_{1p}\exp(-i\delta_1)+r_{2p}\exp(i\delta_1)}{\exp(-i\delta_1)+r_{1p}r_{2p}\exp(i\delta_1)} \exp(-iK_{zo}z)\right|^2 \sin^2\theta_o$$

$$= |\exp(iK_{zo}z) + r_p \exp(-iK_{zo}z)|^2 \sin^2\theta_o$$

The film (1) phase.

$$F_x(z) = \left|\frac{t_{1p}[\exp(-i\delta_1)\exp(iK_{z1}z)-r_{2p}\exp(i\delta_1)\exp(-iK_{z1}z)]\cos\theta_1}{\exp(-i\delta_1) + r_{1p} r_{2p} \exp(i\delta_1)}\right|^2$$

$$= \left|\frac{t_{1p}\,\{\exp[iK_{z1}(z-h_1)]-r_{2p}\exp[-iK_{z1}(z-h_1)]\}\cos\theta_1}{\exp(-i\delta_1) + r_{1p} r_{2p} \exp(i\delta_1)}\right|^2$$

$$F_y(z) = \left|\frac{t_{1s}\,\{\exp[iK_{z1}(z-h_1)]+r_{2s}\exp[-iK_{z1}(z-h_1)]\}}{\exp(-i\delta_1) + r_{1s} r_{2s} \exp(i\delta_1)}\right|^2$$

$$F_z(z) = \left|\frac{t_{1p}\,\{\exp[iK_{z1}(z-h_1)]+r_{2p}\exp[-iK_{z1}(z-h_1)]\}\sin\theta_1}{\exp(-i\delta_1) + r_{1p} r_{2p} \exp(i\delta_1)}\right|^2$$

The substrate (2) phase.

$$F_x(z) = \left|\frac{t_{1p}\,t_{2p}\exp[iK_{z2}(z-h_1)]\cos\theta_2}{\exp(-i\delta_1)+r_{1p}r_{2p}\exp(i\delta_1)}\right|^2 = |t_p \cos\theta_2|^2 \exp[-\beta_2(z-h_1)]$$

$$F_y(z) = \left|\frac{t_{1s}\,t_{2s}\exp[iK_{z2}(z-h_1)]}{\exp(-i\delta_1)+r_{1s}r_{2s}\exp(i\delta_1)}\right|^2 = |t_s|^2 \exp[-\beta_2(z-h_1)]$$

$$F_z(z) = \left|\frac{t_{1p}\,t_{2p}\exp[iK_{z2}(z-h_1)]\sin\theta_2}{\exp(-i\delta_1)+r_{1p}r_{2p}\exp(i\delta_1)}\right|^2 = |t_p \sin\theta_2|^2 \exp[-\beta_2(z-h_1)]$$

can be calculated using the profile of the field along the direction of the depth. Lissberger proposed a formula for the relationship between absorptance and electric field of the radiation in multilayer thin films.[22] In this section, we show another integral formulation for the relationship, which is approximately applicable to the layers with gradient refractive index and extinction coefficient. In general, the total absorptance $A$, which is equal to the emittance in the emission spectrum, is given by

$$A = 1 - R - T, \tag{44}$$

when the final phase or the substrate is transparent, or

$$A = 1 - R, \tag{45}$$

when the substrate is light absorbing. However, from these formulas, we cannot know the contribution from a specific part or layer in the films to the total absorptance. According to Poynting's theorem, the differential absorptance $dA$ in the differential thickness $dz$ is proportional to the intensity of the electric field of the light at the depth $z$;

$$dA = q_j F(z) dz, \tag{46}$$

where the proportional coefficient $q_j$ is given as

$$q_j = \mathrm{Re}\left(\frac{\hat{n}_j \cos\theta_j}{\hat{n}_0 \cos\theta_0}\right)\beta_j \tag{47}$$

$$\beta_j = 2\,\mathrm{Im}(K_{z_j}) = 4\pi\nu\,\mathrm{Im}(\hat{n}_j \cos\theta_j). \tag{48}$$

The subscript $j$ is the number of the layer to which the point at the depth $z$ belongs. The definition of $\beta_j$ is the same as given in Eq. (43). In Eqs. (47) and (48), $\beta_j$ expresses the attenuation of the light along the direction normal to the surface of the films. The partial absorptance of the thickness from an arbitrary depth $z = z_1$ to another depth $z_2$ ($z_1 < z_2$) is

$$A(z_1 < z < z_2) = \int_{z_1}^{z_2} q_j F(z) dz. \tag{49}$$

If the initial phase is transparent as in air or an ATR prism, the proportional coefficient $q_j$ becomes

$$q_j = \frac{n_j \alpha_j}{n_0 \cos\theta_0} \tag{50}$$

$$\alpha_j = 4\pi\nu k_j, \tag{51}$$

since $\mathrm{Re}(\hat{n}_j \cos\theta_j) \times \mathrm{Im}(\hat{n}_j \cos\theta_j) = n_j \times k_j$.[5] The quantity $\alpha_j$ is called the absorption coefficient in the spectroscopic terminology, and expresses the attenuation along the direction of the propagation of the light in the film. Equation (50) is just equal to the coefficient in Harrick's equation originally derived to show the relationship between the absorptance and the electric field intensity of the evanescent wave in ATR spectroscopy.[3] The coefficient described here, however, is quite general, and is valid not only for ATR configurations but also strictly for all kinds of stratified films.

Even if there is a gradient in the refractive index $n(z)$ and the extinction coefficient $k(z)$ along the direction of the depth, we can calculate the approximate partial absorptance using the following equation within the same framework, especially in case of a sufficiently small extinction coefficient.

$$A(z_1 < z < z_2) = \frac{4\pi\nu}{n_0 \cos\theta_0} \int_{z_1}^{z_2} n(z) k(z) F_0(z) dz, \tag{52}$$

where $F_0(z)$ means the unperturbed electric field in which the average and constant values should be used for $k$ and $n$. This equation will be useful, especially in the case where the variation of the $n(z)$ and $k(z)$ values do not have a serious effect on the $F(z)$ value such as in ATR spectroscopy. Carlsson and Wiles,[23] and later Tompkins[24] derived an equation for the absorptance caused by a species distributed nonuniformly for a simple ATR case. Stuchebryukov *et al.*[25] derived an equation dealing with the concentration gradient in a film in a three-phase system. All of these equations can be derived from Eq. (52) as special cases.

We can consider Eqs. (44), (45), (49), and (52) for the absorptance as the formulas for the emittance in emission spectroscopy, based on Kirchhoff's law. This problem will be discussed in the succeeding paper.[18] In that case, the beam intensity formula $I(z)$ defined by the following equation will play an important role, instead of the field intensity formula $F(z)$

$$I(z) = \mathrm{Re}\left(\frac{\hat{n}_j \cos\theta_j}{\hat{n}_0 \cos\theta_0}\right) F(z). \tag{53}$$

## V. Field Analysis for Some Reflection Methods

In this section, we attempt to analyze three different reflection spectroscopic methods utilizing metal surfaces using the present field intensity description. The methods we will mention here are reflection-absorption (RA),[2,6] surface electromagnetic wave (SEW),[13,14] and metal overlayer ATR (MOATR)[12] spectroscopies. We examine, for each method, how the electric field profiles change in the presence or absence of sample, and in the presence or absence of absorption in the sample. Figures 2, 4, and 7 show the dependence of the $z$-component of the electric field at the interface between the sample and metal on the incident angle, for samples with the same thickness for RA, SEW, and MOATR methods, respectively.

For the case of RA, the $F_z(z)$ value changes largely due to the presence of the sample, that is, due to the change of the refractive index of the material at the metal surfaces as exemplified by curves (*a*) and (*b*) in Fig. 2. However, it does not change significantly even if the extinction coefficient becomes larger as shown by curve (*c*) where the extinction coefficient $k$ is increased from zero in curve (*b*) to 0.5 in curve (*c*). The incident angles at the maximum field intensity are close to each other. Figure 3 is the depth profile of the $F_z(z)$ value at the incident angle of 75°, which is the angle usually used for RA measurements. From the figure, we can see that the information from every depth in a sample contributes equally to the resultant spectrum in the RA method.

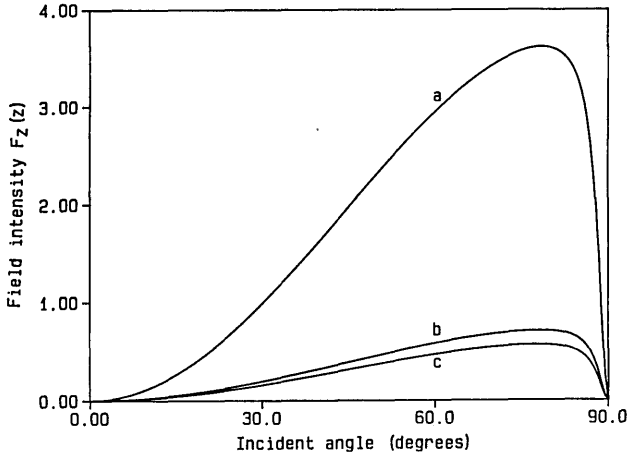


Fig. 2. Angular dependence of the electric field intensity $F_z(z)$ at the surface of the metal for the case of reflection-absorption spectroscopy. The parameters used in the calculation are as follows: $\hat{n}_0 = 1.0, \hat{n}_1 = 1.0\,(a), 1.5\,(b)$, and $1.5 + 0.5i\,(c), \hat{n}_2 = 3.0 + 30.0i, h_1 = 0.01\ \mu\text{m}, \nu = 1000\ \text{cm}^{-1}$.

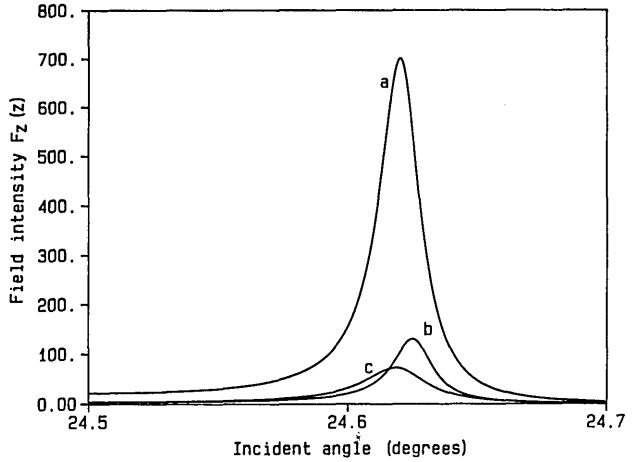


Fig. 4. Angular dependence of the electric field intensity $F_z(z)$ at the surface of the metal for the case of surface electromagnetic wave spectroscopy. The parameters used in the calculation are as follows: $\hat{n}_0 = 2.4, \hat{n}_1 = 1.0, \hat{n}_2 = 1.0\,(a), 1.5\,(b)$, and $1.5 + 0.5i\,(c), \hat{n}_3 = 3.0 + 30.0i, h_1 = 45.76\ \mu\text{m}\,(a), 44.22\ \mu\text{m}\,(b)$, and $38.60\ \mu\text{m}\,(c), h_2 = 0.01\ \mu\text{m}, \nu = 1000\ \text{cm}^{-1}$.

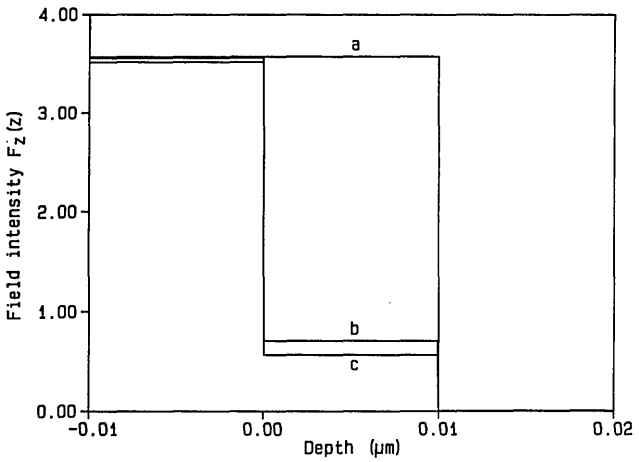


Fig. 3. Depth profile of the electric field intensity $F_z(z)$ at the incident angle of 75° for the case of reflection-absorption spectroscopy. The parameters used in the calculation are as follows: $\hat{n}_0 = 1.0, \hat{n}_1 = 1.0\,(a), 1.5\,(b)$, and $1.5 + 0.5i\,(c), \hat{n}_2 = 3.0 + 30.0i, h_1 = 0.01\ \mu\text{m}, \nu = 1000\ \text{cm}^{-1}$.

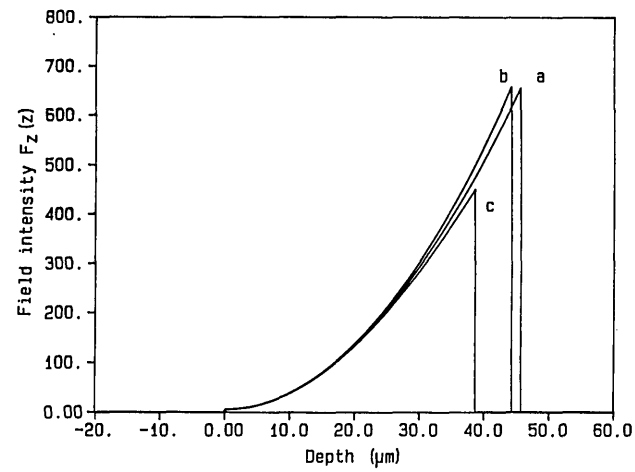


Fig. 5. Depth profile of the electric field intensity $F_z(z)$ at the incident angle of 24.622° (*a*) 24.626° (*b*), and 24.619° (*c*) for the case of surface electromagnetic wave spectroscopy. The parameters used in the calculation are as follows: $\hat{n}_0 = 2.4, \hat{n}_2 = 1.0\,(a), 1.5\,(b)$, and $1.5 + 0.5i\,(c), \hat{n}_3 = 3.0 + 30.0i, h_1 = 45.76\ \mu\text{m}\,(a), 44.22\ \mu\text{m}\,(b)$, and $38.60\ \mu\text{m}\,(c), h_2 = 0.01\ \mu\text{m}, \nu = 1000\ \text{cm}^{-1}$. In this figure, the film thickness for (*b*) or (*c*) is so small that the electric field profile within the film cannot be seen. See Fig. 6.

In the case of SEW, the condition which gives the enhancement of the electric field is severely limited to a narrow range of incident angle as shown in Fig. 4. Moreover, it depends on the refractive index and extinction coefficient. This explains the difficulties met with in selecting the proper experimental conditions in the actual SEW measurements.[13] Figure 5 shows the depth profile of the $F_z(z)$ value for the incident angle which gives the maximum $F_z(z)$ value for each case. This figure depicts the excitement of the surface mode, and shows that this method utilizes the phenomenon of the resonance coupling between the incident and surface waves.[14] However, within the film sample, there is little gradient in the electric field as shown in the expanded depth profile (Fig. 6).

The MOATR method utilizes the enhancement of the electric field intensity due to interference between the incident and reflected waves at the metal surface, similar to the RA method. Here the $F_z(z)$ profile changes depending on both refractive index and extinction coefficient (Fig. 7). Moreover, the incident angle at the maximum $F_z(z)$ value is also shifted. However, the change of the $F_z(z)$ value for each curve is not as steep as for the case of SEW. Figure 8 is the depth profile of the $F_z(z)$ value for the incident angle of 75°. Due to the presence of absorption, the $F_z(z)$ value decreases greatly, but it is still far larger than that for

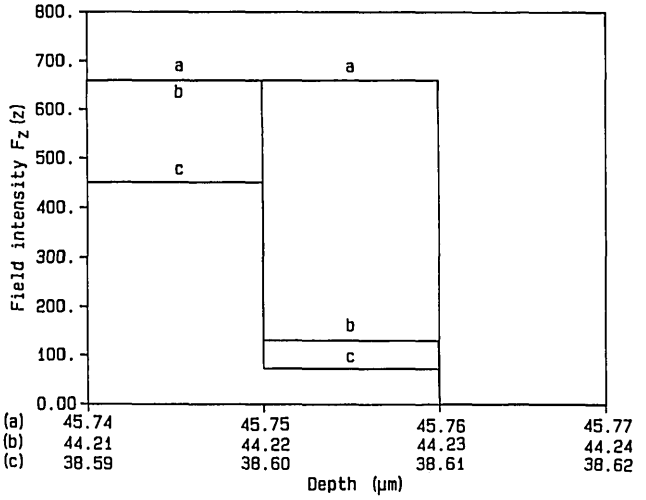


Fig. 6. Expanded depth profile of the electric field intensity $F_z(z)$ around the sample film. The parameters used in the calculation are the same as those in Fig. 5.

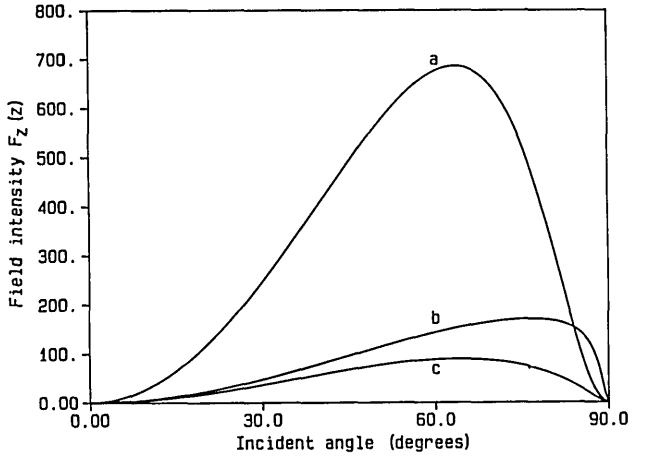


Fig. 7. Angular dependence of the electric field intensity $F_z(z)$ at the surface of the metal for the case of metal overlayer ATR spectroscopy. The parameters used in the calculation are as follows: $\hat{n}_0 = 4.0$, $\hat{n}_1 = 1.0$ (*a*), 1.5 (*b*), and $1.5 + 0.5i$ (*c*), $\hat{n}_2 = 3.0 + 30.0i$, $h_1 = 0.01$ μm, $\nu = 1000$ cm$^{-1}$.

the RA method. These results indicate the high sensitivity and the ease of the selection of the measurement conditions of this method.

For the RA and MOATR methods, the profiles shown here depict only the contribution of the enhancement of the field intensity due to the interference; therefore, we must take into account the enhancement due to the oblique incidence as seen from Eqs. (47) or (50) for the total absorptance.

## VI. Conclusions

In this report, we have introduced a new matrix algorithm to calculate the electric field intensity of the light at an arbitrary depth in a stratified multilayered film. From this general formulation, we can derive several equations which are important in the field of optical spectroscopy. We have tried to apply the results obtained by the presence method to the analysis of three reflectance spectroscopic methods utilizing metal surfaces. In a later paper, we show that a similar matrix method is also applicable to the system with phase incoherency.

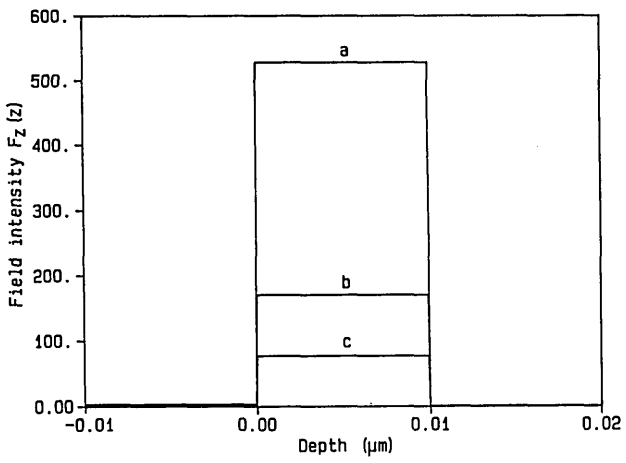


Fig. 8. Depth profile of the electric field intensity $F_z(z)$ at the incidence angle of 75° for the case of metal overlayer ATR spectroscopy. The parameters used in the calculation are as follows: $\hat{n}_0 = 4.0$, $\hat{n}_1 = 1.0$ (*a*), 1.5 (*b*), and $1.5 + 0.5i$ (*c*), $\hat{n}_2 = 3.0 + 30.0i$, $h_1 = 0.01$ μm, $\nu = 1000$ cm$^{-1}$.

The authors gratefully acknowledge the financial support of IBM Corporation. The authors also thank Yuichi Ishino for his valuable comments and suggestions.

## References

1. T. C. Fry, "Plane waves of light. III: Absorption by Metals," J. Opt. Soc. Am. **22**, 307–332 (1932).
2. S. A. Francis and A. H. Ellison, "Infrared Spectra of Monolayers on Metal Mirrors," J. Opt. Soc. Am. **49**, 131–138 (1959).
3. N. J. Harrick, "Electric Field Strengths at Totally Reflecting Interface," J. Opt. Soc. Am. **55**, 851–857 (1965).
4. K. Ohta and R. Iwamoto, "Experimental Proof of the Relation Between Thickness of the Probed Surface Layer and Absorbance in FT-IR-ATR Spectroscopy," Appl. Spectrosc. **39**, 418–425 (1985).
5. W. N. Hansen, "Internal Reflection Spectroscopy in Electrochemistry," in *Advances in Electrochemistry and Electrochemical Engineering*, Volume 9, P. Delahay and C. W. Tobias, Eds. (Wiley, New York, 1973), pp. 1–60.
6. J. D. E. McIntyre, "Specular Reflection Spectroscopy of the Electrode–Solution Interphase," in *Advances in Electrochemistry and Electrochemical Engineering*, Volume 9, P. Delahay and C. W. Tobias Eds. (Wiley, New York, 1973), pp. 61–166.
7. N. M. Bashara and D. W. Peterson, "Ellipsometer Study of Anomalous Absorption in Very Thin Dielectric Films on Evaporated Metals," J. Opt. Soc. Am. **56**, 1320–1331 (1966).
8. M. R. Philpott and J. D. Swalen, "Exciton Surface Polaritons on Organic Crystals," J. Chem. Phys. **69**, 2912–2921 (1978).

9. A. Brillante, M. R. Philpott, and I. Pockrand, "Experimental and Theoretical Study of Exciton Surface Polaritons on Organic Crystals. I. (010) Face of TCNQ$^0$ Single Crystals," J. Chem. Phys. **70,** 5739–5746 (1979).
10. M. Ohsawa, W. Kusakari, and W. Suetaka, "Raman Spectra and Molecular Orientation of 7,7′, 8,8′-Tetracyanoquinodimethane in Thin Films Evaporated on Aluminum," Spectrochim. Acta **36A,** 389–396 (1980).
11. M. Osawa, M. Kuramitsu, A. Hatta, W. Suetaka, and H. Seki, "Electromagnetic Effect in Enhanced Infrared Absorption of Adsorbed Molecules on Thin Metal Films," Sur. Sci. **175,** L787–L793 (1986).
12. Y. Ishino and H. Ishida, "Grazing Angle Metal Overlayer Infrared ATR Spectrscopy," Appl. Spectrosc. **42,** 1296–1302 (1988).
13. Y. Ishino and H. Ishida, "Fourier Transform Infrared Surface Electromagnetic Spectroscopy of Polymer Thin Films on Metallic Substrate," Anal. Chem. **58,** 2448–2453 (1986).
14. Y. Ishino and H. Ishida, "Spectral Simulation of Infrared Surface Electromagnetic Wave Spectroscopy," Sur. Sci., in press (1988).
15. W. N. Hansen, "Electric Fields Produced by the Propagation of Plane Coherent Electromagnetic Radiation in a Stratified Medium," J. Opt. Soc. Am. **58,** 380–390 (1968).
16. F. Abeles, "Recherches sur la Propagation des Ondes Electromagnetiques Sinusoidales dans les Milieux Stratifies. Application aux Couches Minces," Ann. Phys. (Paris) **5,** 596–640 (1950).
17. F. Abeles, "Sur la Propagation des Ondes Electromagnetiques dans les Milieux Stratifies," Ann. Phys. (Paris) **3,** 504–520 (1948).
18. K. Ohta and H. Ishida, "Matrix Formulation for Calculation of Light Beam Intensity in Stratified Multilayered Films and its Application to the Analysis of Emission Spectra," Appl. Opt. (in press).
19. O. S. Heavens, *Optical Properties of Thin Solid Films* (Dover, New York, 1965), Chap. 4.
20. R. M. A. Azzam and N. M. Bashara, *Ellipsometry and Polarized Light* (North-Holland, Amsterdam, 1977), Chap. 4.
21. J. D. Swalen and J. F. Rabolt, "Characterization of Orientation and Lateral Order in Thin Films by Fourier Transform Infrared Spectroscopy," in *Fourier Transform Infrared Spectroscopy,* Volume 4, J. R. Ferraro and L. J. Basile Eds. (Academic, Orlando, FL, 1985), pp. 283–314.
22. J. A. Johnson and D. W. Peterson, "The Relative Electric Fields in a Thin Film on an Opaque Substrate," Sur. Sci. **16,** 217–220 (1969); and P. H. Lissberger, "The Relationship Between Optical Absorptance and Electric Field of the Radiation in Multilayer Thin Films," Opt. Acta **28,** 187–200 (1981).
23. D. J. Carlsson and D. M. Wiles, "Photooxidation of Polypropylene Films. IV. Surface Changes Studied by Attenuated Total Reflection Spectroscopy," Macromolecules **4,** 174–179 (1971).
24. H. G. Tompkins, "The Physical Basis for Analysis of the Depth of Absorbing Species Using Internal Reflection Spectroscopy," Appl. Spectrosc. **28,** 335–341 (1974).
25. S. D. Stuchebryukov, A. A. Vavkushevskii, and V. M. Rudoi, "Frustrated Total Internal Reflection Spectroscopy of Films with Absorption Gradients," Sov. Phys. Dokl. **27,** 931–932 (1982).